J. For. Res. (2023) 34:441–452
https://doi.org/10.1007/s11676-022-01481-6

ORIGINAL PAPER

Effects of water and salt for groundwater-soil systems on root growth and architecture of *Tamarix chinensis* in the Yellow River Delta, China

Jia Sun[1,2] · Ximei Zhao[1] · Ying Fang[1] · Fanglei Gao[1] · Chunhong Wu[1] · Jiangbao Xia[1]

Received: 10 September 2021 / Accepted: 28 December 2021 / Published online: 11 May 2022
© Northeast Forestry University 2022

Abstract To test the patterns of the root morphology and architecture indexes of *Tamarix chinensis* in response to water and salt changes in the two media of the groundwater and soil, three-year-old *T. chinensis* seedlings were chosen as the research object. Groundwater with four salinity levels was created, and three groundwater level (GL) were applied for each salinity treatment to measure the root growth and architecture indexes. In the fresh water and brackish water treatments, the topological index (*TI*) of the *T. chinensis* roots was close to 0.5, and the root architecture was close to a dichotomous branching pattern. In the saline water and saltwater treatments, the *TI* of the *T. chinensis* roots was large and close to 1.0, and the root architecture was close to a herringbone-like branching pattern. Under different GLs and salinities, the total root length was significantly greater than the internal link length, the external link length was greater than the internal link length, and the root system showed an outward expansion strategy. The treatment with fresh water and a GL of 1.5 m was the most suitable for *T. chinensis* root growth, while the root growth of *T. chinensis* was the worst in the treatment with saline water and a GL of 0.3 m. *T. chinensis* can adapt to the changes in soil water and salt by regulating the growth and morphological characteristics of the root system. *T. chinensis* can adapt to high-salt environments by reducing its root branching and to water deficiencies by expanding the distribution and absorption area of the root system.

Keywords Groundwater · Salinity · Soil water and salt · Root system · *Tamarix chinensis* · Topological structure

Project funding: The research was financially supported by the Joint Funds of the National Natural Science Foundation of China (U2006215), the National Natural Science Foundation of China (31770761), the Shandong Key Laboratory of Coastal Environmental Processes, YICCAS (2019SDHADKFJJ16), the Natural Science Foundation of Shangdong Province (ZR2020QD003), and Taishan Scholars Program of Shandong Province, China (TSQN201909152).

The online version is available at http://www.springerlink.com.

Corresponding editor: Yu Lei.

✉ Jiangbao Xia
xiajb@163.com

1 Shandong Key Laboratory of Eco-Environmental Science for the Yellow River Delta, Binzhou University, Binzhou 256600, People's Republic of China

2 College of Forestry, Shandong Agricultural University, Tai'an 271018, People's Republic of China

Introduction

The Yellow River Delta (YRD) in China is an alluvial plain formed by the sediment deposited by the Yellow River in the Bohai Bay Basin and is located at the junction of rivers, sea, and land, with a unique ecosystem and important ecological functions (Zhao et al. 2020). It has multiple dynamic systems, including fresh water and sea water, land and sea, natural and artificial, etc. Ecological interface, and has the youngest, most expansive, and most biologically diverse wetland ecosystem in the global warm temperate zone. The ecosystem has a unique type and has important ecological functions (Zhao 2018). Groundwater level (GL) in the Yellow River Delta is generally shallow, and the salinity of groundwater changes from brackish water to saltwater with the distance from the coastal zone and the influence of the Yellow River flow path changes. Groundwater near the Yellow River banks is mainly freshwater habitats (Cao et al. 2014). In addition, with effect of seawater intrusion, a high precipitation-evaporation ratio, and human activities related to the economy and production, such as shrimp farming and salt harvesting, the secondary salinization of soil in this area is exacerbated; therefore, soil erosion and vegetation degradation are serious and plant growth is compromised. Secondary soil salinization and the distribution of water and salt in soil are closely related to the GL and groundwater salinity (Zhao et al. 2017). An increase in groundwater salinity or a decrease in GL can lead to increased soil moisture content (SMC) and soil salt content (SSC) (Song et al. 2016; Li et al. 2019). Shallow groundwater is the main factor that affects the migration, accumulation, and release of salt. Different groundwater salinities can easily lead to large fluctuations in SMC and SSC, thereby affecting the growth, development, distribution, and succession of vegetation (Kopeć et al. 2013; Fu and Isabela 2015). The joint effect of GL, SMC and SSC is more significant in coastal wetlands and some regions in the YRD than in other regions (Cui et al. 2010; Jeevarathinam et al. 2013). When the groundwater table is shallow, salt in underground water can easily accumulate at the surface through capillary rise, causing different degrees of soil salinization (Fan et al. 2012) and further affecting vegetation growth through the root system.

The root system is the key organ for fixing terrestrial plants in soil and effectively absorbing water and mineral nutrients and plays a critical role in plant adaptability (Shahzad and Amtmann 2017). Due to the impacts of habitat changes and genetic factors, the spatial distribution and morphological characteristics of plant roots have certain plasticity, and roots can form special architectures to improve nutrient and water absorption capacity and enhance viability; this strategy allows plant to adapt to different ecological environments and improves their productivity (Kubilay et al. 2018). Root adaptation strategies vary greatly among different plants with different root architectures (Zeng et al. 2013; Soda et al. 2017). When the GL is relatively shallow, the horizontal roots of *Alhagi sparsifolia* Shap. seedlings quickly expand and tillering increases, and when the GL is deeper, the vertical roots of *A. sparsifolia* develop rapidly to exploit space in the deeper soil layers. *A. sparsifolia* seedlings adapt to increases in groundwater depth mainly through increasing the penetration depth and growth rate of vertical roots (Zeng et al. 2013). With increasing salt stress, the root biomass, length, surface area, and volume of *Corylus heterophylla* × *C. avellan* seedling decrease (Luo et al. 2019). The increase in salinity caused by irrigation leads to a reduction in the number and length of *Olea europaea* L. roots and an increase in root turnover (Soda et al. 2017). Under the influence of seawater intrusion and global change, especially sea-level rise, the effect of groundwater on the growth and distribution of plants in coastal wetlands is increasing. Groundwater depth is sensitive to environmental factors, and groundwater is a major water source during the critical vegetation growth period in saline-alkali soil on muddy coasts (Laversa et al. 2015). The GL is closely related to the water and salt in soil, and the root system is an important organ in the interface between plants and the soil-groundwater environment and can directly respond to soil water and salt changes. To date, the research on the effects of the GL on the root system of plants has mainly focused on arid and semiarid areas (Zeng et al. 2013; Li et al. 2015; Musa et al. 2019); studies on the growth strategies of plant roots adapting to water and salt stress in coastal wetlands are few, and the response patterns of plant roots to groundwater are still unclear. Therefore, there is an urgent need to study the effect of GL and groundwater salinity on plant root growth in the YRD.

Tamarix chinensis, one of the early successional species in the riparian zone, has strong adaptability to floods and high-salt environment and is widely distributed in the wetlands of the YRD. *T. chinensis* has high adaptability and well-developed roots and can regulate salt balance by excreting excessive salt through saline glands. This species can adapt to saline environments. It is the main shrub species used for improving saline-alkaline areas in the YRD and plays an important role in preventing soil erosion, maintaining the stability of reservoir banks, improving soil, and maintaining the balance of coastal wetland ecosystems (Sun et al. 2016). The water and salt conditions in a habitat are the main factors contributing to the growth, distribution, and low quality and low efficiency of *T. chinensis* forests (Xia et al. 2016; Xia et al. 2018). Research on the interaction between *T. chinensis* and groundwater in the YRD has mainly focused on the following three aspects: (1) the distribution characteristics of water and salt of the soil column in areas planted with *T. chinensis* (Song et al. 2016) and the photosynthetic efficiency and water consumption characteristics of T. chinensis (Xia et al. 2017) under different groundwater salinities; (2) the effects of different GLs on the photosynthesis and sap flow of *T. chinensis* (Xia et al. 2018; Ren et al. 2019), the distribution characteristics of soil-*T. chinensis* water contents and salinity (Xia et al. 2016), and the transport characteristics of salt ions in the soil column in areas planted with *T. chinensis* (Zhao 2018) under different GLs; and, (3) the responses of the growth characteristics of *T. chinensis* to the GL and SSC (Cui et al. 2010). Currently, there are few studies on the growth distribution and root architecture of *T. chinensis* in response to different GLs, groundwater salinities and their interaction, and the growth distribution patterns and growth strategies of *T. chinensis* roots under water and salt stress are not clear yet, which, to some extent, affects the maintenance and management of low-efficiency *T. chinensis* forests and water and salt management in *T. chinensis* seedlings.

Therefore, in this study, water with differing salinities (fresh water, brackish water, saline water, and salt water) was created, three GLs (0.3, 0.9, and 1.5 m) were set for each salinity, and the root growth and architecture indexes, such as root diameter, root depth, root biomass, topological index (*TI*) and link length, of three-year-old *T. chinensis* seedlings were measured. The response patterns of the root morphology and architecture of *T. chinensis* to changes in GL and groundwater salinity were investigated to clarify the suitable growth conditions for *T. chinensis*, thus providing a theoretical basis and technical support for water and salt management for *T. chinensis* seedlings in the YRD.

Materials and methods

Materials

This study was carried out in a research greenhouse of the Shandong Key Laboratory of Eco-Environmental Science for the YRD (117° 58′ 57″ E, 37° 22′ 56″ N). The transmittance of the greenhouse glass exceeds 90%, the average indoor air relative humidity is 45% ± 6%, and the average atmospheric temperature is 25 °C ± 4 °C. The experimental soil was taken from a beach on the lower Yellow River. The soil texture is silt loam, with a clay content of 5.76%, a silt content of 47.66%, and a sand content of 46.58%. The soil type is fluvo-aquic soil, with an initial pH value of 7.54, an average SSC of 0.1%, a field water capacity of 37.86%, and a soil bulk density of 1.32 g cm^{-3}. Three-year-old *T. chinensis* seedlings were used in this study.

Experimental design

This study simulated water with four salinities: fresh water (A), salinity of 0 g/L; brackish water (B), salinity of 3 g L^{-1}; saline water (C), salinity of 8 g L^{-1}; and salt water (D), salinity of 20 g L^{-1}. Three GLs were used for each salinity: 0.3, 0.9, and 1.5 m. Three replicates were used for each combination of GL and groundwater salinity, and a total of 36 soil columns were planted with *T. chinensis*.

The experimental design in this study was as follows. In a smart greenhouse, a polyvinyl chloride (PVC) pipe (with an inner diameter of 0.3 m) was used as the container for the planting of *T. chinensis*, and a bucket (height × diameter of the upper mouth × bottom diameter = 0.70 m × 0.57 m × 0.45 m) was used to simulate different GLs and groundwater salinities. To prevent the simulated groundwater from being altered too much due to the ambient temperature and to ensure the uniformity of the groundwater temperature, 0.6 m ditches were dug, and the buckets were embedded in the soil. The design of the PVC pipe container was as follows: (1) according to the formula that PVC pipe height = simulated GL + the actual water depth of 0.55 m + the top interstice layer of 0.03 m, PVC pipe containers with heights of 0.88, 1.48 and 2.08 m were prepared. Multiple 2.0-cm-diameter holes were made around the round PVC pipes according to the soil sampling depth to serve as soil sampling holes; these holes were blocked by plugs. On each PVC pipe in the actual flooded zone (flooding depth at 0.55 m), four 1.0-cm inlets were made every 10 cm and covered with a permeable cloth. The bottom of the PVC pipe in the flooded zone was covered with a permeable cloth and a filtering layer to ensure that the artificial groundwater could fully enter the soil from the bottom and inlets on the sides. (2) After the experimental soil was mixed well, the soil column was filled according to the bulk density of the soil (the depth of one layer was 20 cm), and the soil was compacted one layer at a time. (3) Three-year-old *T. chinensis* seedlings with uniform growth and an average root diameter of 1.40 cm were cut off at 50 cm and planted in the PVC pipes. Three seedlings were planted in each pipe, and fresh water was poured onto the soil surface (4 L/event × 3 events). (4) After 30 days, one seedling was randomly selected from the surviving seedlings in each PVC pipe, the simulated treatments with different GLs and groundwater salinities were performed, and no water was added to the soil surface. To maintain the stability of the GL and groundwater salinity, the GL and salinity of the simulated groundwater were examined every 3 days during the entire experimental period, and the corresponding amounts of water and salt were added if needed. For each soil column, the soil water and salt parameters and root growth parameters (such as TI) of the planted *T. chinensis* seedling were measured from July 8, 2017, to July 20, 2017 (810 days after the start of treatments). A schematic diagram of the soil column and photo of the experiment are shown in Fig. 1.

Determination of indexes and methods

Soil water and salt parameters

For the soil columns in which *T. chinensis* were planted, soil samples were taken one layer at a time (with each layer being 20 cm). Three samples were randomly selected from each round PVC pipe. The SMC was determined by the oven drying method, the SSC was measured by the residue drying method, and the soil to water ratio was 5:1. The absolute concentration of the soil solution (%) = SSC (proportion to dry soil mass)/SMC (proportion to dry soil mass) × 100%.

Root growth parameters of T. chinensis

In total, 36 *T. chinensis* plants were collected. The sediment attached to the roots was rinsed with tap water, and the following parameters were measured with tools, such as a Vernier caliper and meter stick: (1) the numbers of internal and external root links and link lengths; (2) the

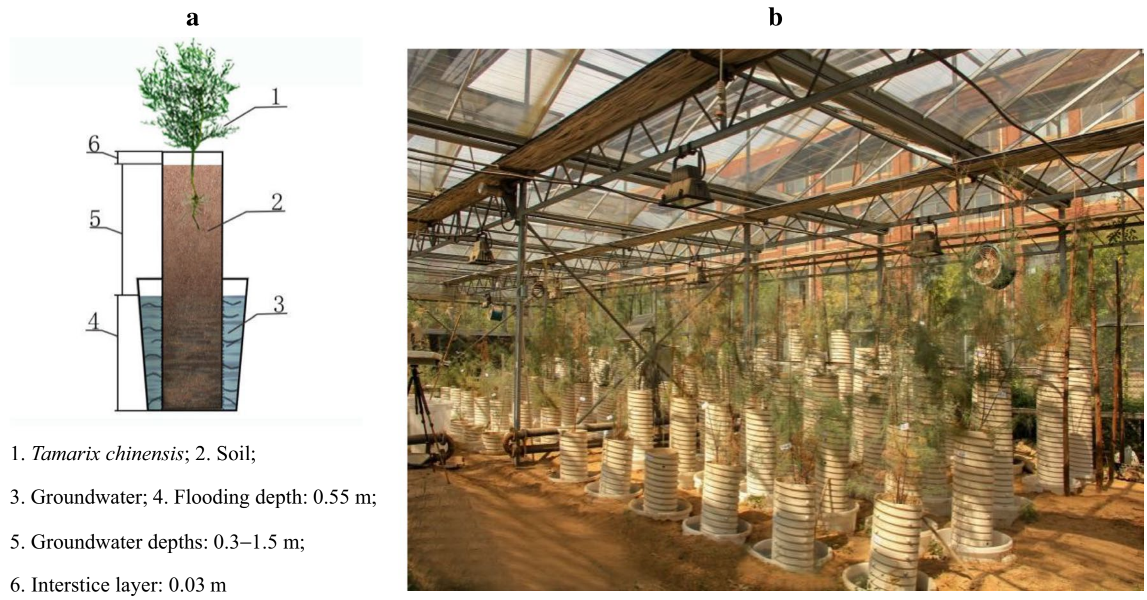

Fig. 1 Schematic diagram (**a**) and photo of soil columns (**b**) with planted *T. chinensis* under different groundwater levels and mineralization treatments

root diameter for each root class and root length; and, (3) the number of root classes and the root biomass. The root biomass was measured as follows: the roots were first dried at 105 °C, then after 30 min, the roots were dried at 80 °C to a constant weight, and the fresh weight and dry weight of each part were measured.

Root topological structure

Bouma et al. (2001) and Fitter et al. (1991) proposed two extreme root topological structures, i.e., a dichotomous branching pattern and herringbone-like branching pattern, and used *TI* to reflect the branching patterns of different plant root systems. The formula for calculating *TI* is:

$$TI = \frac{lgA}{lgM} \quad (1)$$

where, M is the total number of external links of the root system and A is the total number of internal links in the longest path of the root system. When $TI = 1$, the root system belongs to the herringbone-like branching pattern, and when $TI = 0.5$, the root system belongs to the dichotomous branching pattern (Fig. 2).

Data analysis

Excel 2010 and Origin 8.0 were used for data processing and plotting. SPSS 20.0 statistical software was used to perform two-way analysis of variance (ANOVA) on the soil water and salt parameters and root indexes for different treatments,

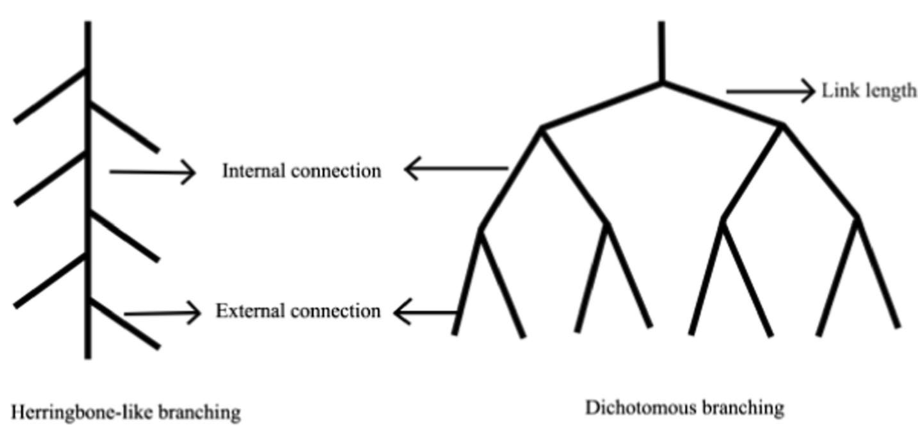

Fig. 2 The schematic view of topology of root system

and multiple comparisons were performed using Duncan's test.

Results

Soil water and salt parameters of soil columns planted with *T. chinensis*

Table 1 shows that GL, groundwater salinity and their interaction had significant effects on the SSC ($P<0.01$). In the saltwater treatment, when the GL was 0.3 m, the SSC reached its maximum value (0.61%). With increasing groundwater salinity, the SSC increased significantly. In the brackish water, saline water, and saltwater treatments, the SSCs were 3.30, 4.56, and 7.83 times that of fresh water, respectively. With increasing GL, the SSC gradually decreased, and the most significant decline in SSC occurred in the saline water treatment. The GL had an extremely significant impact on the SMC ($P<0.01$). With increasing GL, the SMC significantly decreased; when the GL was 0.9 m and 1.5 m, the SMC decreased by 16.28% and 60.06%, respectively, compared to that when the GL was 0.3 m,. The effect of groundwater salinity on the SMC was not significant ($P>0.05$). The effects of GL, groundwater salinity, and their interaction on the absolute concentration of soil solution were extremely significant ($P<0.01$). With increasing groundwater salinity, the absolute concentration of soil solution significantly increased ($P<0.01$). In the brackish water, saline water, and saltwater treatments, the absolute concentration of the soil solution was 3.53, 4.27, and 10.06 times that in the freshwater treatment, respectively. With increasing GL, the absolute concentration of the soil solution showed an increasing trend (Fig. 3).

Root growth indexes of *T. chinensis*

The root diameter of *T. chinensis* varied significantly with different groundwater salinities ($P<0.01$). The root diameter of *T. chinensis* in the brackish water, saline water and saltwater treatments was significantly lower than that in the freshwater treatments, by 21.51%, 25.77%, and 42.51%, respectively. With increasing GL, the root diameter of *T. chinensis* first increased and then decreased. In the freshwater treatment, when the GL was 0.9 m, *T. chinensis* root diameter reached its maximum (32.70 mm) (Table 2, Fig. 4a).

Table 2 and Fig. 4b show that the GL significantly affected the root depth of *T. chinensis* ($P<0.01$). With increasing GL, the root depth of *T. chinensis* significantly increased. When the GL was 1.5 and 0.9 m, the root depth of *T. chinensis* was 2.49 and 1.98 times that observed when the GL was 0.3 m, respectively. There were no significant differences in the root depth of *T. chinensis* under different groundwater salinities ($P>0.05$). Both GL and groundwater salinity significantly affected the number of lateral roots of *T. chinensis* ($P<0.01$). With increasing GL, the number of *T. chinensis* lateral roots increased in the fresh water, brackish water, and saltwater treatments, but first increased and then decreased in the saline water treatment. With increasing groundwater salinity, the number of *T. chinensis* lateral

Table 1 Two-way ANOVA results of groundwater levels and groundwater salinity on the water-salt parameters of planted *T. chinensis* soil columns

	df	Soil salt content	Soil moisture content	Soil solution absolute content
Groundwater salinity	3,24	353.62**	2.42^{ns}	84.36**
Groundwater level	2,24	53.74**	126.575**	10.83**
Groundwater salinity × Groundwater level	6,24	3.89**	1.06**	5.73**

**$P<0.01$; *$P<0.05$; ns $P>0.05$

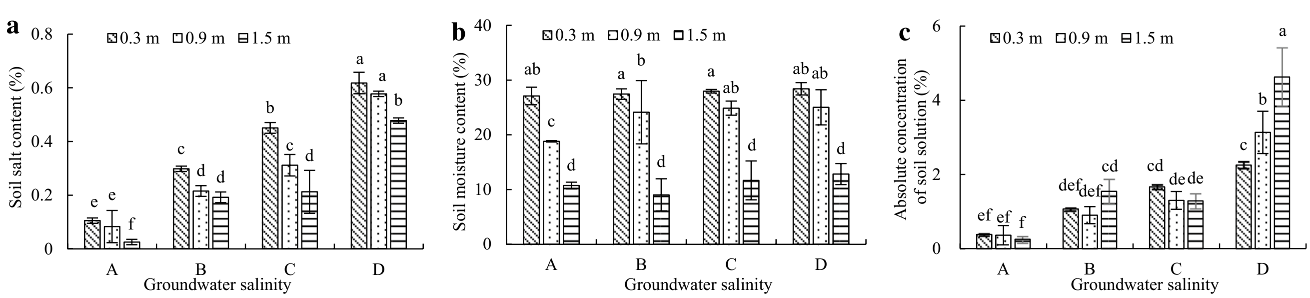

Fig. 3 Water and salt parameters of soil columns planted with *T. chinensis* under different groundwater levels and mineralization treatments

roots significantly decreased. When the GL was 0.3 m, the number of *T. chinensis* lateral roots of in the brackish water, saline water, and saltwater treatments decreased by 25.23%, 62.61%, and 59.81% compared to that in the freshwater treatment, respectively (Fig. 4c). The interaction between the GL and groundwater salinity showed no significant effect on the root growth parameters of *T. chinensis* ($P > 0.05$).

Root biomass of *T. chinensis*

Groundwater salinity significantly affected the taproot biomass of *T. chinensis* ($P < 0.01$). The taproot biomass of *T. chinensis* in the brackish water, saline water, and saltwater treatments was significantly lower than that in the freshwater treatment, with the decreases of 32.70%, 25.67%, and 70.08%, respectively (Table 3, Fig. 5a). The first-order lateral root biomass of *T. chinensis* was significantly different under different salinities and different GLs ($P < 0.01$), and in the saltwater treatment, the biomass was reduced by 61.22% compared to that in the freshwater treatment. With the increase in GL, the first-order lateral root biomass of *T. chinensis* increased significantly. When the GL was 0.9 and 1.5 m, the first-order lateral root biomass was 1.24 and 2.21 times that when the GL was 0.3 m, respectively (Table 3, Fig. 5b). Groundwater salinity, GL, and their interaction all significantly affected the second-order lateral root biomass of *T. chinensis* ($P < 0.01$). With increasing GL, the second-order lateral root biomass of *T. chinensis* gradually increased in the fresh water, brackish water, and saltwater treatments and first increased and then decreased in the saline water treatment. When the GL was 0.9 m and 1.5 m, the second-order lateral root biomass of *T. chinensis* was 2.59 and 3.33 times that at GL = 0.3 m, respectively. The second-order lateral root biomass of *T. chinensis* in the brackish water and saltwater treatments was significantly lower than that in the freshwater treatment, with decreases of 51.00% and 61.00%, respectively. In the freshwater treatment, when the GL was 1.5 m, the second-order lateral root biomass of *T. chinensis* reached its maximum (69.17 g) (Fig. 5c). Groundwater salinity and GL had a significant impact on

Table 2 Two-way ANOVA results of groundwater levels and groundwater salinity on the growth indexes of *T. chinensis* root system

	df	Root diameter	Root depth	Lateral root number
Groundwater salinity	3,24	0.36^{ns}	30.00**	24.30**
Groundwater level	2,24	7.66**	0.69^{ns}	8.80**
Groundwater salinity × Groundwater level	6,24	0.993^{ns}	0.73^{ns}	1.70^{ns}

**$P < 0.01$; *$P < 0.05$; ns $P > 0.05$

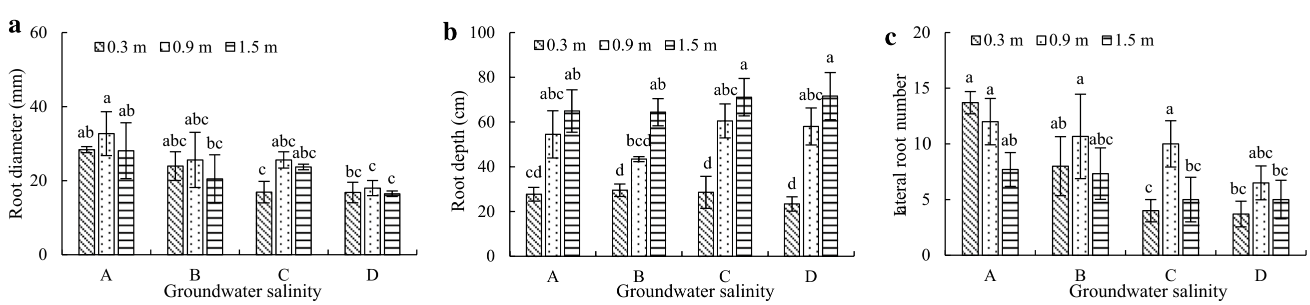

Fig. 4 *T. chinensis* root diameter (**a**), root depth (**b**), and lateral root number (**c**) under different groundwater levels and salinity treatments

Table 3 Two-way ANOVA results of groundwater levels and groundwater salinity on the *T. chinensis* root biomass

	df	Taproot biomass	First-order lateral root biomass	Second-order lateral root biomass	Capillary root biomass
Groundwater salinity	3,24	0.72^{ns}	6.70**	15.83**	3.32*
Groundwater level	2,24	14.65**	3.44*	8.28**	5.60**
Groundwater salinity × Groundwater level	6,24	0.88^{ns}	0.25^{ns}	6.48**	0.38^{ns}

**$P < 0.01$; *$P < 0.05$; ns $P > 0.05$

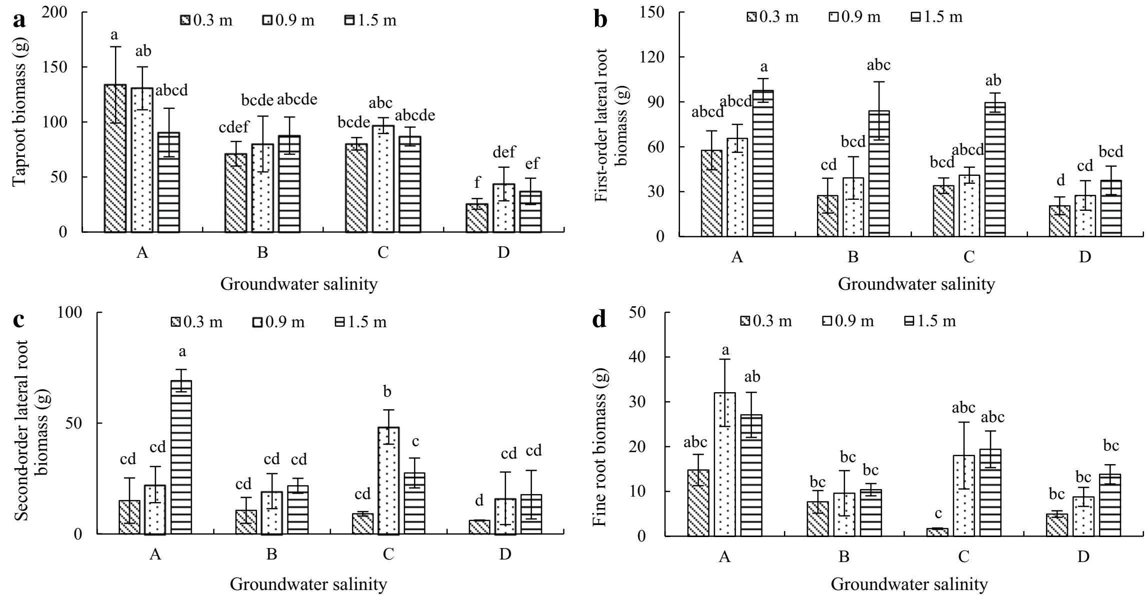

Fig. 5 *T. chinensis* taproot biomass (**a**), first-order lateral root biomass (**b**), second-order lateral root biomass (**c**), and capillary root biomass (**d**) under different groundwater levels and mineralization treatments

Table 4 Two-way ANOVA results of groundwater levels and groundwater salinity on the *T. chinensis* root system topological index and root system length

	df	Topological index	Link length	Total root length
Groundwater salinity	3,24	2.76*	37.66**	10.78**
Groundwater level	2,24	1.35^{ns}	12.09*	8.75**
Groundwater salinity × Groundwater level	6,24	0.97^{ns}	0.70^{ns}	0.72^{ns}

$^{**}P<0.01$; $^{*}P<0.05$; ns $P>0.05$

the capillary root biomass of *T. chinensis* ($P<0.05$), but the effect of their interaction was not significant ($P>0.05$). The fine root biomass of *T. chinensis* in the brackish water, saline water, and saltwater treatments was significantly lower than that in the freshwater treatment, by 60.60%, 47.08% and 62.72%, respectively. The fine root biomass of *T. chinensis* increased with increasing GL but decreased with increasing groundwater salinity.

Topological structure of *T. chinensis* roots

The root system *TI* can reflect the differences in the root topological structures of *T. chinensis* under different GLs and groundwater salinities. Under different groundwater salinities, the *TI* of *T. chinensis* roots was significantly different ($P<0.05$) (Table 4). The average TI of the *T. chinensis* roots decreased in the descending order of fresh water, brackish water, saline water and salt water. In the fresh water and brackish water treatments (i.e., those with relatively low salinity), the *TI* of the *T. chinensis* roots was small and close to 0.5, indicating that the structure of the root branches was

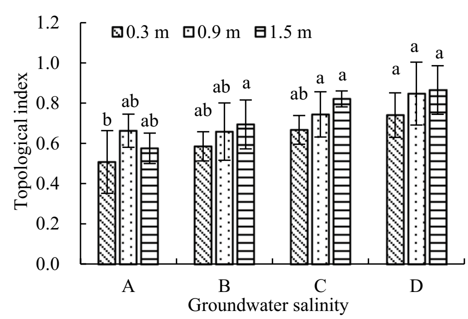

Fig. 6 Topological index of *T. chinensis* root system under different groundwater levels and mineralization treatments

complex and close to a dichotomous branching pattern. In the saline water and saltwater treatments, which have a relatively high salinity, the *TI* of the *T. chinensis* roots was large and close to 1.0, indicating that the structure of the root branches was relatively simple and close to a herringbone-like branching pattern (Fig. 6). The GL and the interaction between GL and groundwater salinity showed no significant impact on the root topographical structure of *T. chinensis* ($P > 0.05$).

Root length of *T. chinensis*

GL and groundwater salinity had a significant impact on the root link length of *T. chinensis* ($P < 0.05$) (Table 4). With the increase in groundwater salinity, the root link length of *T. chinensis* first increased and then decreased, reaching its maximum in the brackish water treatment, which indicates that saline water and salt water, which have relatively high salinity, had a certain inhibitory effect on the root link length of *T. chinensis*. With the increase in GL, the root link length of *T. chinensis* gradually increased. When the GL was 0.9 and 1.5 m, the root link length was 1.37 and 1.95 times than that when the GL was 0.3 m, respectively (Fig. 7a).

GL and groundwater salinity had an extremely significant impact on the total root length of *T. chinensis* ($P < 0.01$) (Table 4). The total root length of *T. chinensis* decreased significantly in the brackish water, saline water, and saltwater treatments, with decreases of 46.72%, 53.39% and 60.33% compared to that in the freshwater treatment, respectively. With increasing GL, the total root length of *T. chinensis* gradually increased. In the freshwater treatment, when the GL was 0.9 and 1.5 m, the total root length of *T. chinensis* increased by 30.14% and 110.57% compared to that when the GL was 0.3 m, respectively (Fig. 7b).

Discussion

Influence of groundwater salinity on root growth and architecture of *T. chinensis*

With increasing groundwater salinity, both the SSC and SMC showed an upward trend. Higher groundwater salinity favors the rise of salt due to the capillary effect. The groundwater salinity was extremely significantly positively correlated with the SSC and the absolute concentration of the soil solution ($P < 0.01$), but the correlation the between groundwater salinity and SMC was not significant ($P > 0.05$). In the saline water and saltwater treatments, which had relatively high salinity levels, the diameter and number of lateral roots of *T. chinensis* significantly decreased, and the high-salt environment inhibited increases in root diameter and the number of lateral roots. However, some studies have found that under water and salt stress, the number of lateral roots of different plants could significantly increase or decrease; this difference might be related to the fact that some factors, such as plants, saltwater stress intensity, and salt type, differ between studies (Li et al. 2010; Xu et al. 2020). To adapt to changes in the external environment, plants can adjust the allocation pattern of biomass to optimize resource allocation (Lloret et al. 1999); in particular, the biomass changes in taproots, first-order lateral roots, second-order lateral roots, and fine roots play an important role in soil fixation by roots, nutrient uptake by roots, and plant growth and development (Zhu et al. 2018). With the increase in groundwater salinity, the SSC and the absolute concentration of soil solution significantly increased, while the overall biomass of the taproots, first-order lateral roots, second-order lateral roots, and fine roots of *T. chinensis* exhibited a downward trend. The biomass of the taproots and fine roots of *T. chinensis* was extremely significantly negatively correlated with the groundwater salinity ($P < 0.01$) (Table 5), indicating that high-salt conditions had a certain inhibitory effect on the growth of the taproots, lateral roots, and fine roots of *T. chinensis*, which might lead to a decrease in soil fixation and nutrient uptake by and metabolism of *T. chinensis* roots. The root system is the main part of the plant to absorb salt. In order to ensure the continued growth of *T. chinensis* in a high-salt environment, the root biomass is reduced to reduce the absorption of salt, which in turn makes the salt ion transport relatively slow, effectively avoiding salt stress damage (Zhang 2013). The freshwater treatment provided the most suitable condition for root growth in *T. chinensis*. The total root biomass was the highest (250.09 g ind.$^{-1}$) in the freshwater treatment, followed by the saline water (180.80 g ind.$^{-1}$) and brackish water (155.26 g ind.$^{-1}$) treatments, while that in the saltwater treatment was the lowest (83.13 g ind.$^{-1}$). The salt stress caused by high-salinity groundwater significantly reduced the root growth indexes

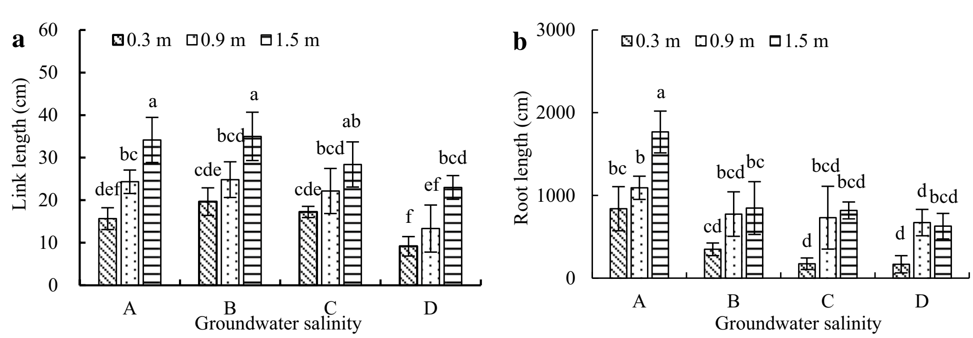

Fig. 7 *T. chinensis* root system link length (**a**) and total root length (**b**) under different groundwater levels and mineralization treatments

Table 5 Correlation coefficient of the root system index and environmental factors

	Groundwater level	Groundwater salinity	Soil moisture content	Soil salt content	Soil solution absolute content
Groundwater level	1				
Groundwater salinity	0	1			
Soil moisture content	− 0.914**	− 0.072	1		
Soil salt content	− 0.297	0.929**	0.175	1	
Soil solution absolute content	0.186	0.805**	− 0.312	0.758**	1
Root diameter	− 0.042	− 0.637**	0.185	− 0.601**	− 0.574**
Root depth	0.805**	0.020	− 0.696**	− 0.235	0.112
Lateral root number	− 0.095	− 0.558**	0.217	− 0.496**	− 0.423*
Taproot biomass	− 0.023	− 0.695**	0.123	− 0.704**	− 0.587**
First-order lateral root biomass	0.489**	− 0.414*	− 0.460**	− 0.557**	− 0.287
Second-order lateral root biomass	0.504**	− 0.322	− 0.440**	− 0.459**	− 0.250
Capillary root biomass	0.114	− 0.482**	0	− 0.513**	− 0.421*
Topological index	0.243	0.373*	− 0.231	0.249	0.191
Link length	0.736**	− 0.432**	− 0.676**	− 0.621**	− 0.228
Total root length	0.520**	− 0.521**	− 0.471**	− 0.628**	− 0.334*

*$P < 0.05$; **$P < 0.01$

and belowground biomass of *T. chinensis*, which was not conducive to dry matter accumulation (Zhang et al. 2017). However, the taproot biomass of *Phragmites australis* in the YRD is not significantly affected by the SSC (Tian et al. 2019), indicating that the adaptability of different plants to salt stress varies significantly.

Root topological structure can determine the spatial distribution characteristics of plant roots, has an important impact on nutrient uptake and soil fixation by roots, and can, to some extent, reflect the root foraging strategies of plants in different habitat conditions, especially the competitiveness of the lateral roots in acquiring nutrients (Paz et al. 2015). Fitter et al. (1991) proposed using the *TI* to reflect the root architecture and dividing the root architecture into two extreme types: a herringbone-like branching pattern and a dichotomous branching pattern. For the herringbone-like branching pattern ($TI = 1.0$), all the branches are directly connected to the taproot, are external branches, and do not continue to branch. For the dichotomous branching pattern ($TI = 0.5$), two branches at each branching point produce secondary branches with the same angle and number. However, due to factors such as plant biological characteristics, soil nutrients, and soil mechanical resistance, the actual root architecture falls between these two patterns (Fang et al. 2019). In the fresh water and brackish water treatments, which had a relatively low salinity, the SSC and the absolute concentration of soil solution were both low, the water and salt conditions were suitable, the root length of *T. chinensis* increased, and the root architecture was close to the dichotomous branching pattern, which is a root network structure formed mainly by the expansion of the distribution range of the root system and addition of secondary branches. For the dichotomous branching pattern, the root branches are abundant, but the expansion distance of the roots is short per unit of resource input; therefore, this root branching pattern is more suitable for soil environments with relatively rich resources (He et al. 2016). In the saline water and saltwater treatments, with relatively high salinity levels, the SSC and the absolute concentration of soil solution were both relatively high. Due to the high salinity, the root length of *T. chinensis* was reduced, the root architecture was close to the herringbone-like branching pattern, and the root *TI* and groundwater salinity were extremely significantly positively correlated ($P < 0.01$) (Table 5). SSC can inhibit the conversion and accumulation of nutrients in the soil. Moreover, the reduction in soil enzyme activities under high-salt conditions can inhibit microbial activity, leading to nutrient-poor soil (Xie et al. 2015) and resulting in a significantly elevated root *TI*. Under high groundwater salinity conditions, *T. chinensis* can harvest resources by decreasing the number of root branches and increasing the root expansion distance per unit of resource input (He et al. 2016), which is consistent with the results of a study by Bouma et al. (2001).

Root link length and root length showed extremely negative correlations with groundwater salinity ($P < 0.01$) (Table 5). As the groundwater salinity increased, the SSC increased, the increase in the root length of *T. chinensis* decreased, and the root link length of *T. chinensis* decreased significantly. To minimize the toxicity from high SSCs, *T. chinensis* adopted an avoidance mechanism, i.e., reducing the distribution range of the roots. As salt stress increased, the root length of *Corylus heterophylla* × *C. avellan* seedlings decreased (Luo et al. 2019), which is consistent with the results of this study.

Influence of GL on the root growth and architecture of *T. chinensis*

When the GL was 0.3 m, the root depth of *T. chinensis* under different groundwater salinities was only 27.30 cm. When approaching groundwater, the root system could turn or branch to avoid the hypoxic environment caused by flooding or salinity stress, which is consistent with the results of research on responses of *Robinia pseudoacacia* and *Fraxinus chinensis* Roxb. roots to water and salt conditions on muddy coasts (Zhang et al. 1992). With the increase of groundwater depth, seedlings of *Populus euphratica* seedlings increase rooting depth and increase root biomass to adapt to drought stress environments to maintain their requirements for soil moisture and nutrients (Ding et al., 2021). However, when the GL is too deep and plant roots cannot reach the zones in which they can obtain water through capillary rise, plants can be affected by water deficiency (Liu et al. 2021). There was a highly significantly negative correlation between the GL and SMC ($P < 0.01$) and a negative correlation between the GL and SSC (Table 5). As the GL increased, the SMC and SSC decreased significantly (Table 1, Fig. 2), and the root diameter of *T. chinensis* first increased and then decreased, reaching its maximum when the GL was 0.9 m. At high GLs, *T. chinensis* roots absorbed water in deep soil layers by decreasing the root diameter. Tsakaldimi et al. (2009) found that to resist drought, naturally growing oak (*Quercus ilex*) seedlings would extend taproots deep into wet soil at the cost of inhibiting the growth of the root diameter, which is conducive to supplying energy for the longitudinal growth of taproots and enhancing the absorption and utilization of water and nutrients in deep soil. When *A. sparsifolia* grows in an environment with a deep GL, the vertical roots develop rapidly to exploit space in the deeper soil layers (Zeng et al. 2013; Li et al. 2015). The seedlings of *Populus euphratica* can utilize deep soil moisture through the longitudinal expansion of vertical roots (Lv et al. 2015). Increasing vertical root growth can significantly increase water uptake, which is conducive to the use of groundwater resources for maintaining the survival and growth of seedlings in the dry season. In the sea-side plot, *Pinus thunbergii* has a plate root systems with thicker and longer horizontal roots, but fewer tap roots were observed, whereas tap root systems were well developed in the land-side plots, where the groundwater level was deeper (Hirano et al. 2018). It can be seen that the adaptability of different plant species to the habitat also shows a certain degree of consistency. However, some studies have shown that the distribution of the root system of *T. chinensis* in the coastal area of the YRD tends to be shallow, exhibiting horizontal root characteristics (Song et al. 2017), while in sandy habitats formed from seashells, the proportion of vertical roots of *T. chinensis* is the largest and the root depth is large (Zhao et al. 2015), indicating that the root system of *T. chinensis* has strong plasticity and adaptability to changes in water and salt conditions. In this study, from the perspective of effective nutrient space, in the root distribution of *T. chinensis* under different GLs and groundwater salinities, the proportion of vertical roots was significantly larger than that of horizontal roots. In the field, the horizontal space for the growth of *T. chinensis* roots is large; however, in this study, the horizontal space for root growth of *T. chinensis* was restricted by the PVC pipe diameter. In this study, *T. chinensis* roots could grow only in the vertical direction (as indicated by the increased distribution of vertical roots) to increase the space they occupied, thus increasing their nutrient space.

Lateral roots can increase the total root biomass, root length, and root surface area, and lateral roots are the most active part of the root system (Rewald et al. 2011). The first- and second-order lateral root biomass of *T. chinensis* showed a highly significantly positive correlation with the GL ($P < 0.01$) and a highly significantly negative correlation with the SMC and SSC (Table 5). In the treatment with a high GL and low SMC and SSC, *T. chinensis* was able to absorb sufficient water for plant growth by increasing its lateral root biomass. When the water supply is deficient, the root system often has a well-developed lateral root system (Fenta et al. 2014), which promotes the uptake of water and nutrients in deep soil, helping to maintain photosynthesis (Comas et al. 2013). When the GL was 1.5 m, the total root biomass of *T. chinensis* reached its maximum (197.18 g ind.$^{-1}$). The SMC at this GL was the most suitable for the root growth of *T. chinensis*, followed by a GL of 0.9 m (174.71 g ind.$^{-1}$), and the total root biomass reached its lowest when the GL was 0.3 m (130.07 g ind.$^{-1}$).

Root length has an important impact on the spatial expansion and nutrient uptake capacity of root systems in the soil, and increasing the root link length is one of the important strategies for increasing the spatial distribution of a plant and improving the nutrient uptake capacity (Zeng et al. 2013). The total root length and the root link length of *T. chinensis* were highly significantly positively correlated with the GL and significantly negatively correlated with the SMC and SSC ($P < 0.01$) (Table 5). With increasing GL, the total root length and root link length of *T. chinensis* showed an increasing trend. In this way, *T. chinensis* can enhance its spatial expansion ability in the deep soil to adapt to environments with relatively low SMC and SSC values and cover more water and nutrient space to meet its growth needs. Under different GLs and different groundwater salinities, the total root length of *T. chinensis* was far greater than the internal root link length of *T. chinensis*, and the external root link length of *T. chinensis* was greater than the internal root link length of *T. chinensis*, suggesting that the *T. chinensis* root system exhibited an outward expansion strategy. This is consistent with the results of studies on plant root architecture characteristics in karst peak-cluster depression areas (Su et al. 2018) and the Taklamakan Desert region (Guo et al. 2014), indicating that it is a common root growth strategy to have external root link lengths greater than internal root link lengths.

Conclusion

GL, groundwater salinity and their interaction can significantly affect soil water and salt changes. Groundwater salinity mainly affects SSC and the absolute concentration of soil solution, while the GL mainly affects the SSC and SMC. The GL and groundwater salinity had a significant impact on the root growth of *T. chinensis*, but the effect of their interaction was not significant.

T. chinensis mainly adopted an avoidance mechanism to adapt to the high-salinity environment by reducing root diameter, number of lateral roots, root biomass, link length, and root length. *T. chinensis* increased distribution range and absorption area to adapt to water deficiency. In the fresh water and brackish water treatments, which had relatively low salinity levels, the topological structure of the *T. chinensis* was close to a dichotomous branching pattern. In the saline water and saltwater treatments, which had relatively high salinity levels, the topological structure of the *T. chinensis* was close to a herringbone-like branching pattern. Under different GLs and different groundwater salinities, the total root length of *T. chinensis* was far greater than the root link length of *T. chinensis*, and the external root link length of *T. chinensis* was greater than the internal root link length of *T. chinensis*, suggesting that the root system of *T. chinensis* exhibited an outward expansion strategy.

Our study can provide the groundwater-soil aspect for in-depth studies of the relationship between the root architecture of *T. chinensis* and soil water and salt, and a technical reference for water and salt management in the *T. chinensis* forest along mud coasts. From the perspective of the total root biomass of *T. chinensis*, the combination of fresh water and a GL of 1.5 m was the most suitable for the root growth of *T. chinensis*. The worst root growth occurred in the treatment with salt water and a GL of 0.3 m. The *T. chinensis* root growth was better in the saline water than in the brackish water, and the worst root growth occurred in salt water. Avoid planting *T. chinensis* seedlings under high groundwater levels (GL < 0.3 m) and high salinity conditions in salt water, which is not conducive to the growth and development of their roots. *T. chinensis* can adapt to the changes in soil water and salt caused by different GLs and groundwater salinities by regulating root growth and morphological characteristics, showing strong plasticity and adaptability to different water and salt conditions.

References

Bouma TJ, Nielsen KL, Vanhal J (2001) Root system topology and diameter distribution of species from habitats differing in inundation frequency. Funct Ecol 15(3):360–369

Cao JR, Xu YX, Yu HJ, Huang C (2014) Research on the variation and evolution of groundwater chemistry in the Yellow River Delta. Mar Sci 38(12):78–85

Comas LH, Becker SR, Cruz VMV, Byne PE, Dierig DA (2013) Root traits are contributing to plant productivity under drought. Front Plant Sci 4:442

Cui BS, Yang QC, Zhang KJ, Zhao XS, You ZY (2010) Responses of saltcedar (*Tamarix chinensis*) to water table depth and soil salinity in the Yellow River Delta, China. Plant Ecol 209:279–290

Ding XX, Zhao CY, Zeng Y, Ma XF (2021) Impact of groundwater depth and soil texture on root growth and architecture of *Populus euphratica* seedling. J Soil Water Conserv 35(5):235–241

Fan X, Pedroli B, Liu G, Liu Q, Liu H, Shu L (2012) Soil salinity development in the Yellow River Delta in relation to groundwater dynamics. Land Degrad Dev 23:175–189

Fang H, Rong H, Hallett PD, Mooney SJ, Zhang WJ, Zhou H, Peng XH (2019) Impact of soil puddling intensity on the root system architecture of rice (*Oryza sativa* L.) seedlings. Soil till Res 193:1–7

Fenta BA, Beebe SE, Kunert KJ, Burridge JD, Barlow KM, Lynch PJ, Foyer C (2014) Field phenotyping of soybean roots for drought stress tolerance. Agronomy 4(3):418–435

Fitter AH, Stickland TR, Harvey ML, Wilson GW (1991) Architectural analysis of plant root systems architectural correlates of exploitation efficiency. New Phytol 118:375–382

Fu BH, Isabela B (2015) Riparian vegetation NDVI dynamics and its relationship with climate, surface water and groundwater. J Arid Environ 113:59–68

Guo JH, Zeng FJ, Li CJ, Zhang B (2014) Root architecture and ecological adaptation strategies in three shelterbelt plant species in the southern Taklimakan Desert. Chin J Plant Ecol 38(1):36–44

He GZ, Chen YN, Chen YP, Wang RZ (2016) Adaptive strategy of *Tamarix* spp root architecture in arid environment. J Beijing Norm Univ (nat Sci) 52(3):277–282

Hirano Y, Todo C, Yamase K, Tanikawa T, Dannoura M, Ohashi M, Doi R, Wada R, Ikeno H (2018) Quantification of the contrasting root systems of *Pinus thunbergii* in soils with different groundwater levels in a coastal forest in Japan. Plant Soil 426:327–337

Jeevarathinam C, Rajasekar S, Miguel AFS (2013) Vibrational resonance in groundwater-dependent plant ecosystems. Ecol Complex 15(5):33–42

Kopeć D, Michalska-Hejduk D, Krogulec E (2013) The relationship between vegetation and groundwater levels as an indicator of spontaneous wetland restoration. Ecology 57(8):242

Kubilay Y, Adem Y, Seda S, Sumeyye T (2018) Responses of grapevine rootstocks to drought through altered root system architecture and root transcriptomic regulations. Plant Physiol Bioch 127:256–268. https://doi.org/10.1016/j.plaphy.2018.03.034

Laversa DA, Hannahb DM, Bradleyb C (2015) Connecting large-scale atmospheric circulation, river flow and groundwater levels in a chalk catchment in southern England. J Hydrol 523(1):179–189

Li WR, Zhang SQ, Ding SY, Shan L (2010) Root morphological variation and water use in alfalfa under drought stress. Acta Ecol Sin 30(19):30–40

Li CJ, Zeng FJ, Zhang B, Liu B, Guo ZC, Gao HH, Tashpolat T (2015) Optimal root system strategies for desert phreatophytic seedlings in the search for groundwater. J Arid Land 7(4):462–474

Li XQ, Xia JB, Zhao XM, Chen YP (2019) Effects of planting *Tamarix chinensis* on shallow soil water and salt content under different groundwater depths in the Yellow River Delta. Geoderma 335:104–111

Liu SS, Xu GQ, Li Y, Wu X, Liu J, Mi XJ (2021) Difference and consistency of responses of five sandy shrubs to changes in groundwater level in the Hailiutu River Basin. Acta Ecol Sin 41(2):1–11

Lloret F, Casanovas C, Penuelas J (1999) Seedling survival of Mediterranean shrubland species in relation to root shoot ratio, seed size and water and nitrogen use. Funct Ecol 13(2):210–216

Luo D, Shi YJ, Song FH, Li JC (2019) Effects of salt stress on growth, photosynthetic and fluorescence characteristics, and root architecture of *Corylus heterophylla* × *C. avellan* seedlings. Chin J Appl Ecol 30(10):3376–3384

Lv X, Zhang XH, Zhang N, Xia YG, Jing JL, Li JW (2015) Response of root growth and architecture of *Populus euphratica* seedling on soil water. Acta Bot Boreal -Occident Sin 35(5):1005–1012

Musa A, Zhang Y, Cao J, Wang YC, Liu Y (2019) Relationship between root distribution characteristics of Mongolian pine and the soil water content and groundwater table in Horqin Sandy Land, China. Trees 33:1203–1211

Paz H, Pineda-García F, Pinzón-Pérez LF (2015) Root depth and morphology in response to soil drought: comparing ecological groups along the secondary succession in a tropical dry forest. Oecologia 179(2):554–561

Ren RR, Xia JB, Zhang SY, Zhao ZG, Zhao XM (2019) Response characteristics of photosynthesis and sap flow parameters in *Tamarix chinensis* leaves to depth of groundwater table in the Yellow River Delta. J Nat Resour 34(12):2615–2628

Rewald B, Ephrath JE, Rachmilevitch S (2011) A root is a root is a root? Water uptake rates of Citrus root orders. Plant Cell Environ 34(1):33–42

Shahzad Z, Amtmann A (2017) Food for thought: how nutrients regulate root system architecture. Curr Opin Plant Biol 39:80–87

Soda N, Ephrath JE, Dag A, Beiersdorf I, Presnov E, Yermiyahu U, Alon BG (2017) Root growth dynamics of olive (*Olea europaea* L.) affected by irrigation induced salinity. Plant Soil 411:305–318

Song ZC, Xia JB, Zhao XM, Zhang GD, Li CZ, Bi YQ (2016) Distribution characteristics of soil moisture and salinity in the soil columns with planting *Tamarix chinensis* under different groundwater mineralization. Sci Soil Water Conserv 14(2):41–48

Song XJ, Li SN, Wei W, Guo J, Yu YL, Liu ZW (2017) Distribution characteristics of root f system of *Tamarix chinensis* in Yellow River Delta and its influence factors. Wetl Sci 15(5):716–723

Su L, Du H, Wang H, Zeng FP, Song TQ, Peng WX, Chen L, Zhang F (2018) Root architecture of the dominant species in various vegetation restoration processes in Karst Peak-Cluster depression. Acta Bot Boreal -Occident Sin 38(1):150–157

Sun LK, Liu WQ, Liu GX (2016) Temporal and spatial variations in the stable carbon isotope composition and carbon and nitrogen contents in current-season twigs of *Tamarix chinensis* Lour. and their relationships to environmental factors in the Laizhou Bay wetland in China. Ecol Eng 90:417–426

Tian XY, Chen M, Lu F, Wang AD, Han GX, Guan B (2019) Response of growth and root biomass of *Phragmites australis* to water level and salt stress at different growth stages in the Yellow River Delta. Chin J Ecol 38(2):404–411

Tsakaldimi M, Tsitsoni T, Ganatsas P, Zagas T (2009) A comparison of root architecture and shoot morphology between naturally regenerated and container-grown seedlings of *Quercus ilex*. Plant Soil 324(1–2):103–118

Xia JB, Zhang SY, Zhao XM, Liu JH, Chen YP (2016) Effects of different groundwater depths on the distribution characteristics of soil-*Tamarix* water contents and salinity under saline mineralization conditions. CATENA 142:166–176

Xia JB, Zhao XM, Ren JY, Lang Y, Qu FZ, Xu H (2017) Photosynthetic and water physiological characteristics of *Tamarix chinensis* under different groundwater salinity conditions. Environ Exp Bot 138:173–183

Xia JB, Ren JY, Zhao XM, Zhao FJ, Yang HJ, Liu JH (2018) Threshold effect of the groundwater depth on the photosynthetic efficiency of *Tamarix chinensis* in the Yellow River Delta. Plant Soil 433(1):157–171

Xie WJ, Zhang YP, Zhang M, Li R, Wu LF, Ouyang Z (2015) Relationship between soil physicochemical properties and wheat production in coastal saline soil. Acta Pedol Sin 52(2):461–466

Xu FF, Yan YJ, Wei RX (2020) Effects of NaCl and Na_2CO_3 stress on growth of rice root. Hybrid Rice 35(3):76–78

Zeng FJ, Song C, Guo HF, Liu B, Luo WC, Gui DW, Arndt S, Guo DL (2013) Responses of root growth of *Alhagi sparsifolia* Shap. (Fabaceae) to different simulated groundwater depths in the southern fringe of the Taklimakan Desert, China. J Arid Land 5(2):220–232

Zhang L (2013) Purification effect and physiological and biochemical response of salt-tolerant plants on saline waste water. Zhejiang Ocean University, pp 35–36

Zhang JC, Hu HB, Li DJ (1992) Root research on the main afforestation tree species on the littoral region in northern Jiangsu Province. J Nanjing for Univ 1:35–40

Zhang X, He KN, Shi CQ, Xu T, Wang H, Tang D (2017) Effect of salt stress on growth and physiological characteristics of *Tamarix chinensis* and *Nitraria tangutorum* seedlings. J Northwest a&f Univ 45(1):105–111

Zhao XM (2018) Effects of simulated groundwater on water and salt characteristics of soil-*Tamarix Chinensis* and tamarisk growth in the Yellow River Delta. Shandong Agricultural University, pp 76–78

Zhao YY, Lu ZH, Xia JB, Liu JT (2015) Root architecture and adaptive strategy of 3 shrubs in Shell Bay in Yellow River Delta. Acta Ecol Sin 35(6):1688–1695

Zhao XM, Xia JB, Chen WF, Chen YP (2017) Effect of groundwater depth on the distribution of water and salinity in the soil-*Tamarix chinensis* system under evaporation conditions. Acta Ecol Sin 37(18):6074–6080

Zhao QQ, Bai JH, Gao YC, Zhao HX, Zhang GL, Cui BS (2020) Shifts of soil bacterial community along a salinity gradient in the Yellow River Delta. Land Degrad Dev 3116:2255–2267

Zhu TX, Gao K, Wang L, Gao Y (2018) Effect of root pruning radius and time on root biomass and horizontal distribution in *Helianthus tuberosus*. Pratacult Sci 35(6):1510–1516

Publisher's Note Springer Nature remains neutral with regard to jurisdictional claims in published maps and institutional affiliations.